

Application of the improved cavitation model to turbulent cavitating flow in fuel injector nozzle



Bařış Biçer^{a,b,*}, Akira Sou^{a,1}

^a Graduate School of Maritime Sciences, Kobe University, 5-1-1, Fukaeminami, Higashinada, 658-0022 Kobe, Hyogo, Japan

^b Softflow Co., Ltd., Tama Center Tosei Bldg. 4F, 1-15-2 Ochiai, Tama-shi, Tokyo, Japan

ARTICLE INFO

Article history:

Received 7 May 2015

Revised 3 November 2015

Accepted 26 November 2015

Available online 12 December 2015

Keywords:

Nozzle cavitation

Fuel injector

Critical pressure

Bubble dynamics

Numerical simulation

OpenFOAM

ABSTRACT

Cavitation phenomenon occurring inside diesel injector nozzles plays a key role in atomization of fuel spray. The most common approach to numerically model the cavitating flow is Volume-Of-Fluid (VOF) method, which employs the governing equations for a perfect gas-liquid mixture often in combination with a transport equation for liquid or gas volume fraction. A mass transfer model is required to evaluate the phase change between liquid and vapor. Most of the mass transfer models use the simplest bubble dynamics model, Rayleigh (R) equation which is sometimes called simplified Rayleigh-Plesset (RP) equation, to simulate the growth and collapse of bubbles based on the vapor saturation pressure P_v . We have found that R equation over-predicts cavitation when local pressure is slightly below P_v . We have proposed the Modified Rayleigh (MR) equation taking into account the critical pressure P_c , and showed its validity in some simple test cases with uniform pressure. In this study, the applicability of the MR equation to turbulent cavitating flows in a fuel injector nozzle is examined. OpenFOAM is used for the numerical simulation of turbulent cavitating flows in an one-side rectangular nozzle whose images have been captured by a high-speed camera and the turbulent velocity has been measured by a Laser Doppler Velocimetry (LDV). Turbulent effect is taken into account using RNG k- ϵ model. The numerical results are compared with the experimental data and the turbulent recirculation flow, re-entrant jet and cloud cavitation shedding are well simulated by the MR model.

© 2015 Elsevier Inc. All rights reserved.

1. Introduction

Turbulent cavitating flow in fuel injector nozzles for diesel engines has been widely investigated, since it plays a key role in atomization characteristics of fuel spray which strongly affects diesel engine performance and emissions. A large variety of experimental works have been performed to clarify the influence of cavitation in injector nozzles. An early experimental work was performed by Bergwerk [1], who showed that cavitation results in large amplitude of disturbance which enhances jet atomization. Nurick [2] carried out lots of cavitation experiments using various types of nozzles with different sizes. Hiroyasu et al. [3] showed that spray atomization is improved by the extension of cavitation to the exit of injector nozzle. Soteriou and Andrews [4] investigated the internal cavitating flow structure in a scaled-up nozzle and classified the cavitation into three distinct regions, i.e., a separated boundary layer inner region, a main stream flow, and an attached boundary layer inner region.

* Corresponding author at: Softflow Co., Ltd., Tama Center Tosei Bldg. 4F, 1-15-2 Ochiai, Tama-shi, Tokyo, Japan. Tel.: +81 80 3854 0340; fax: 81 78 431 6294.

E-mail addresses: bicerbaris@hotmail.com, 103w204w@stu.kobe-u.ac.jp (B. Biçer), sou@maritime.kobe-u.ac.jp (A. Sou).

¹ Tel.: +81 78 431 6294; fax: +81 78 431 6294.

Nomenclature

C_c	condensation rate constant
C_v	vaporization rate constant
D_0	nuclei diameter (μm)
\mathbf{U}	mixture velocity (m/s)
K	cavitation number
k	turbulent kinetic energy (m^2/s^2)
l	characteristic length (mm)
L_n	nozzle length (mm)
n_0	bubble number density ($1/\text{m}^3$)
P	pressure (Pa)
t_n	nozzle thickness (mm)
V_n	mean velocity (m/s)
V_{in}	inlet velocity (m/s)
R	radius (μm)
R_c	condensation source term
R_e	evaporation source term
W_n	nozzle width (mm)

Greek symbols

ν	kinematic viscosity (m^2/s)
Δt	time step (s)
Δx	cell size in direction of velocity (mm)
α	volume fraction
ρ	fluid density (kg/m^3)
μ	dynamic viscosity (Pa.s)
σ	surface tension (N/m)
ε	turbulent dissipation rate (m^2/s^3)

Subscripts

0	initial
a	atmospheric
b	bubble
c	critical
eff	effective
in	injector
G	gas
L	liquid
m	mixture
out	outlet
t	turbulence
v	vapor
y	y-direction

Sou et al. [5] observed that cavitation inception takes place as bubble clouds in the recirculation zone near the inlet of a nozzle. The generation of a long cavitation film forms the development of cavitation zone almost to the exit (supercavitation), and shedding of cavitation clouds accompanied in vortices finally induces a large deformation of the liquid jet.

A large number of experimental studies have been conducted using large-scale transparent nozzles, which enable to facilitate clear visualization of cavitation structure and LDV measurement [5–9]. Although important and useful knowledge has been obtained from the experimental attempts, the real effects of the turbulent cavitating flows in injector nozzles remain still unknown due to the refraction of light at the cylindrical side wall of the nozzles, tiny scale of the nozzle of about 0.1 mm in diameter and 1 mm in length, operating at high injection pressure and high velocity up to hundreds meters per second in the nozzles, and complexity of the turbulent cavitating flow. These difficulties also make the experimental visualizations and measurements extremely difficult. Therefore, lots of numerical models have been developed for many years in the literature to simulate cavitation inside injector nozzles [9–26].

In the numerical modeling of the turbulent cavitating flows inside injector nozzles, it is necessary to precisely describe gas or liquid fraction and the resulting change in the mixture fluid properties. Homogeneous Equilibrium Model (HEM) is one of the well-known and widely used multiphase approach due to its simplicity [10,19–24]. This model treats the cavitating flow as a

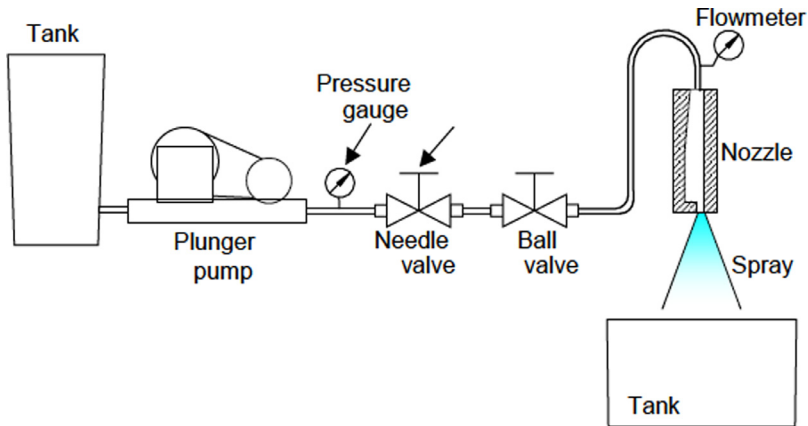


Fig. 1. Experimental apparatus [9].

homogeneous mixture of gas and liquid in a computational cell. One set of the governing equations for the mixture phase are solved, and it takes short computational time. This model presumes the local kinetic and mechanical equilibrium of free Gibbs enthalpy between phases, which corresponds to the equality of the local velocity, temperature and pressure for both phases. **This assumption in homogeneous (equilibrium) models corresponds to ignorance of the thermodynamics effects and also energy equation as well.**

Barotropic equation, which indicates the relation between density and static pressure, is one of the common approaches in HEM for the prediction of growth and collapse of cavitation [10,25,26]. This approach **ignores the bubble dynamics which describes cavitation bubble growth and collapse. Hence, its applicability to the simulation of the nozzle cavitation is limited** [24].

Another approach in HEM to close the system is Mass Transfer Model (MTM). This model solves the transport equation for liquid or gas fraction. MTM based on HEM is commonly called Volume-Of-Fluid (VOF) method in the literature. However, it should be noted that the original VOF method treats a sharp gas-liquid interface in a cell by interface reconstruction and does not treat two-phase mixture [27]. Source terms for MTM are often evaluated by a bubble dynamics model. Yuan et al. [11], Schnerr and Sauer [12], and Zwart et al. [15] computed the bubble growth and collapse in the source terms of the transport equation according to R equation [28], which is a simplified form of Rayleigh-Plesset (RP) equation ignoring the viscous term, surface tension, non-condensable gas, and high-order terms. Singhal et al. [13] used R equation for the transport equation of three-phases. We found out in our previous study [29] that R equation over-estimates cavitation since cavitation takes place when the local pressure is less than the vapor saturation pressure P_v instead of the critical pressure P_c . We proposed the modified Rayleigh (MR) model taking into account P_c , whose prediction is confirmed analytically to agree well with RP prediction. However, the applicability of MR model to cavitation simulation in CFD has not been examined yet. Also, most of previous CFD applications based on RANS model cannot predict the cavitation cloud shedding which enhances the liquid atomization [9].

The objective of the present study is to examine the applicability of MR equation to turbulent cavitating flows in a fuel injector nozzle based on MTM. Simulations are carried out using OpenFOAM software package. RNG k- ϵ model is used as a turbulence model, which is known to applicable to the flow with separation and reattachment. Numerical results are compared with the experimental results [9] in terms of cavitation length, thickness and cavitation cloud shedding behavior in an one-side rectangular nozzle.

2. Experimental setup

Our previous experimental result is used for the validation [9]. Fig. 1 displays the schematic drawing of the experimental setup. A plunger pump discharged filtered tap water through a rectangular nozzle into ambient air. A flow meter was used to measure the liquid flow rate. Fig. 2 shows geometry of the one-side rectangular nozzle used in the experiment, where W_n , L_n and t_n show the nozzle width (1.94 mm), length (8.00 mm) and thickness (1.94 mm), respectively. Stainless steel thin flat plates were used to produce the side walls of the nozzle and a sharp-edge was formed at the inlet of the nozzle. Transparent acrylic flat plates were used for the front and back walls of the nozzle. A digital camera (Nikon, D70, 3008 × 2000 pixels) and a flash lamp (Nissin Electronic, MS-1000 and LH-15M, duration = 4 μ s) were employed to take the images of cavitation and liquid jets. Time evolution of cavitation were captured using a high-speed digital video camera (Redlake, Motion Pro HS-1, frame rate = 20,000 fps, exposure time = 50 μ s) and a reflector lamp (Panasonic, PRF-500). The more details about experimental setup can be found in our previous study [9].

Photos of cavitation and the jets are displayed in Fig. 3. Cavitation and liquid jets are observed as dark color due to the backlight illumination. The cavitation number K and the liquid Reynolds number Re_n are calculated as follows.

$$K = \frac{P_a - P_v}{0.5 \rho_L V_n^2}, \quad (1)$$

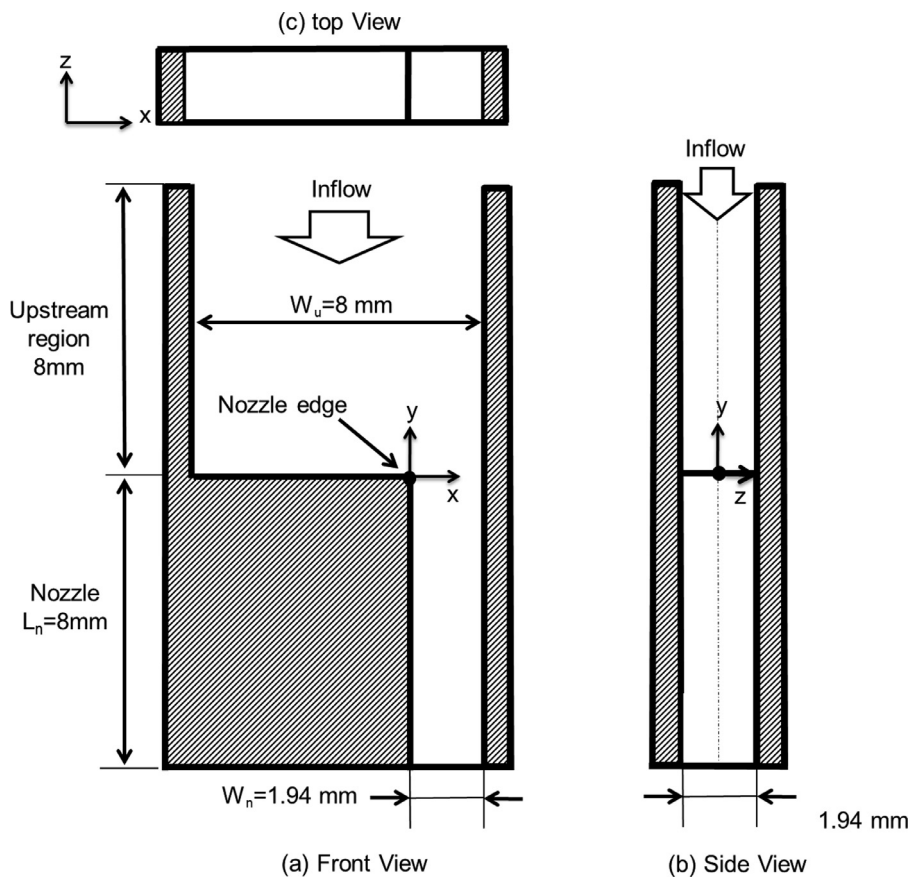


Fig. 2. Nozzle geometry [9].

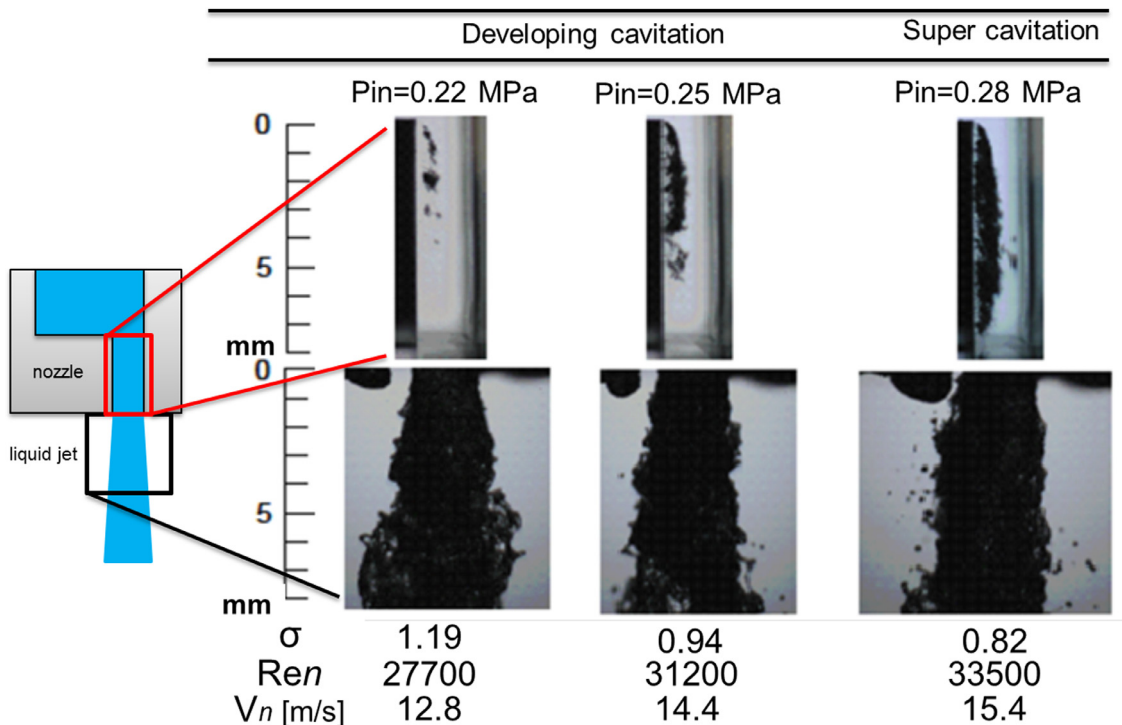


Fig. 3. Cavitation inside nozzle and liquid jet near the nozzle exit [9].

$$\text{Re}_n = \frac{V_n W_n}{\nu_L}, \quad (2)$$

where P_a , P_v , V_n and ν_L denote the atmospheric pressure, vapor saturation pressure, mean liquid velocity in the nozzle and liquid kinematic viscosity, respectively. Calculated cavitation and Reynolds numbers are indicated below the Fig. 3.

3. Numerical model

3.1. Two-phase flow modeling

In order to model the turbulent cavitating flow, two-phase treatment is needed to be determined with the mechanism of the phase transformation between liquid and gas. In this work, a homogenous equilibrium two-phase mixture method (HEM) is used, which supposed that liquid and vapor are perfectly mixed in each cell and one set of conservation equations are solved for the mixture phase. To specify the phase change between liquid and vapor, the following transport equation based on liquid volume fraction α_L is used.

$$\frac{\partial(\alpha_L \rho_L)}{\partial t} + \nabla \bullet (\alpha_L \rho_L \mathbf{U}) = R_c + R_e, \quad (3)$$

where \mathbf{U} , R_c and R_e show mixture velocity, rate of mass transfer source terms for condensation and evaporation, respectively. The density and viscosity of the mixture phase are calculated based on the volume fraction of the liquid phase as follows:

$$\rho_m = (1 - \alpha_L) \rho_v + \alpha_L \rho_L, \quad (4)$$

$$\mu_m = (1 - \alpha_L) \mu_v + \alpha_L \mu_L, \quad (5)$$

where ρ_m and μ_m are the density and viscosity of mixture phase, while ρ_v , ρ_L , μ_v and μ_L represent vapor and liquid densities and dynamic viscosities, respectively. The continuity (mass conservation) is given for the mixture phase by:

$$\frac{\partial \rho_m}{\partial t} + \nabla \bullet (\rho_m \mathbf{U}) = 0. \quad (6)$$

By substituting Eq. (3) into Eq. (6), the mass conservation can be rewritten in the form of velocity divergence as:

$$\nabla \bullet \mathbf{U} = -\frac{1}{\rho_m} \frac{d \rho_m}{dt} = \frac{\rho_L - \rho_v}{\rho_m} \frac{d \alpha_L}{dt}. \quad (7)$$

This shows that divergence velocity field is no longer zero. If Eq. (7) is put into Eq. (3), the mass transfer source terms can be obtained as:

$$R_c + R_e = \frac{\rho_L \rho_v}{\rho_m} \frac{d \alpha_L}{dt}. \quad (8)$$

Regarding to mass transfer source terms definition in Eq. (8), the continuity equation can be written subject to the source terms as follows:

$$\nabla \bullet \mathbf{U} = (R_c + R_e) \left(\frac{1}{\rho_L} - \frac{1}{\rho_v} \right). \quad (9)$$

The momentum equation is written for the mixture phase:

$$\frac{\partial \rho_m \mathbf{U}}{\partial t} + \nabla \bullet (\rho_m \mathbf{U} \mathbf{U}) = -\nabla P + \nabla \bullet [(\mu_{eff} (\nabla \mathbf{U} + (\nabla \mathbf{U})^T)] + \rho_m g, \quad (10)$$

where g shows gravity and μ_{eff} is the effective viscosity and given by:

$$\mu_{eff} = \mu_m + \mu_t, \quad (11)$$

where μ_m and μ_t denote the molecular and turbulence viscosities. The latter is modeled by one of the RANS turbulence model such as RNG k- ϵ model.

3.2. Cavitation model

To specify sources terms in the RHS of the transport Eq. (3), the cavitation model based on bubble dynamics developed by Schnerr and Sauer [12] is chosen due to widely use in the literature [30–36]. In this approach, the volume fraction of vapor phase α_G is given by:

$$\alpha_G = 1 - \alpha_L = \frac{\frac{4}{3}\pi R_b^3 n_0}{1 + \frac{4}{3}\pi R_b^3 n_0}, \quad (12)$$

where R_b and n_0 denote the bubble radius and bubble nuclei number density (the number of nuclei per unit volume), respectively. R_b is represented in terms of n_0 as:

$$R_b = \left(\frac{3\alpha_G}{4\pi(1 - \alpha_G)n_0} \right)^{1/3}. \quad (13)$$

By taking derivative of Eq. (12), we can obtain the derivative of α , which is used in the RHS of Eq. (8).

$$\frac{d\alpha_L}{dt} = -\frac{3\alpha_L(1 - \alpha_L)}{R_b} \frac{dR_b}{dt}. \quad (14)$$

According to Schnerr and Sauer model [12], bubble growth and collapse are calculated by using Rayleigh (R) equation [28],

$$\frac{dR_b}{dt} = \text{sgn}(P_v - P_L) \sqrt{\frac{2|P_v - P_L|}{3\rho_L}}, \quad (15)$$

where P_L is the local liquid pressure. R equation takes vapor saturation pressure P_v as threshold for evaporation and condensation. By using R equation mass transfer rates are given as:

$$\begin{aligned} R_e &= -C_v \frac{3\rho_L \rho_v}{\rho_m} \frac{\alpha_L(1 - \alpha_L)}{R_b} \text{sgn}(P_v - P_L) \sqrt{\frac{2|P_v - P_L|}{3\rho_L}}, & P_L < P_v \\ R_c &= C_c \frac{3\rho_L \rho_v}{\rho_m} \frac{\alpha_L(1 - \alpha_L)}{R_b} \text{sgn}(P_L - P_v) \sqrt{\frac{2|P_v - P_L|}{3\rho_L}}, & P_v < P_L, \end{aligned} \quad (16)$$

where C_v and C_c are the rate constants for condensation and vaporization, respectively and they are set to be 1 for calculations as original values taken from Schnerr and Sauer model [12]. However, we found out in our previous study [29] that R equation over-estimates bubble growth since cavitation takes place when the local pressure is less than the vapor saturation pressure P_v instead of critical pressure P_c . To avoid this overestimation and precisely model the cavitation inside injector nozzle, the MR equation based on the critical pressure P_c is used.

3.3. Critical pressure approach

If the local liquid pressure P_L around a bubble falls below the following pressure threshold, the bubble starts to grow explosively. This pressure threshold is called the critical pressure P_c and given by [37]:

$$P_c = P_v - \frac{4\sigma}{3R_c}, \quad (17)$$

where σ shows surface tension and R_c is the critical bubble radius given by:

$$R_c = R_0 \left[3 \left(\frac{P_{in} - P_v}{2\sigma} R_0 + 1 \right) \right]^{1/2}, \quad (18)$$

where P_{in} denotes the injector pressure and R_0 is the initial bubble diameter. Bubble collapse in Schnerr-Sauer model is also driven by R equation. However, the bubble collapse speed is faster than the bubble growth speed. Therefore, R equation is slightly modified for the bubble collapse by changing the constant 2/3 to 1.27 [29]. Finally, mass transfer rates based on P_c are given as,

$$\begin{aligned} R_e &= -C_v \frac{3\rho_L \rho_v}{\rho_m} \frac{\alpha_L(1 - \alpha_L)}{R_b} \text{sgn}(P_c - P_L) \sqrt{\frac{2|P_v - P_L|}{3\rho_l}}, & P_L < P_c \\ R_e &= R_c = 0, & P_c < P_L < P_v \\ R_c &= C_c \frac{3\rho_L \rho_v}{\rho_m} \frac{\alpha_L(1 - \alpha_L)}{R_b} \text{sgn}(P_L - P_c) \sqrt{1.27 \frac{|P_v - P_L|}{\rho_l}}, & P_v < P_L. \end{aligned} \quad (19)$$

As seen in Eqs. (17) and (18), the critical pressure P_c depends on the injection pressure P_{in} and the initial radius R_0 of the bubble nuclei. The relationship between P_c and nuclei diameter $D_0 (= 2R_0)$ is shown in Fig. 4 for a water injection case with the injection pressure of $P_{in} = 0.22$ MPa. As seen in Fig. 4, P_c does not change a lot for $D_0 \geq 2 \mu\text{m}$. For the all the present simulations, R_0 is set to 1 μm and n_0 is set to 10^{14} m^{-3} . It should be noted that nuclei do not grow at or slightly below P_v but start to grow when $P_L < P_c$ and start to collapse when $P_v < P_L$.

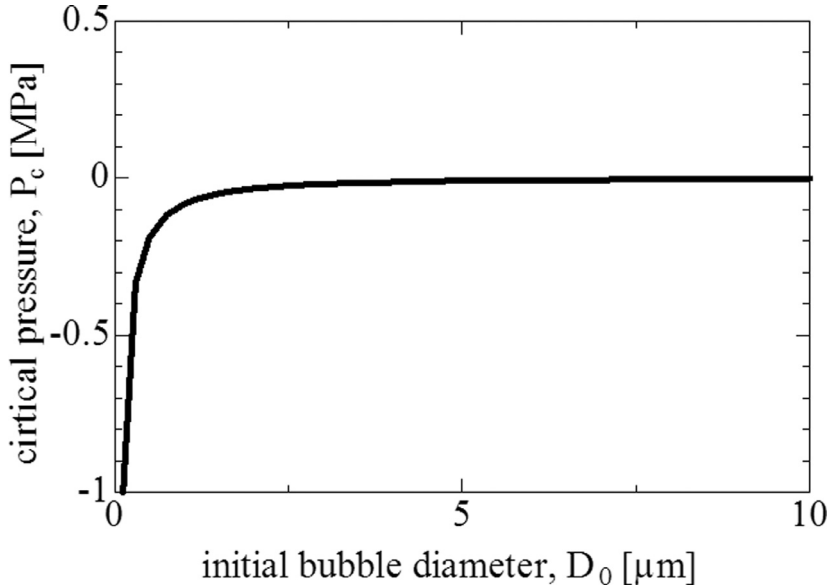


Fig. 4. Critical pressure P_c variation subject to initial bubble diameter D_0 at $P_{in} = 0.22$ MPa.

Table 1
Properties of the different meshes.

	Coarse mesh	Middle mesh	Fine mesh
Total mesh number	32,300	73,100	190,270
Minimum mesh size	100 μm	50 μm	25 μm
CPU time	1 day	2.5 days	4.5 days
y^+	18.1	9	4.5

3.4. RNG $k-\varepsilon$ turbulence modeling

To represent the turbulence effects in the simulations, RNG $k-\varepsilon$ turbulence model proposed by Yakhot et al. [38] is used. This model is derived from conventional $k-\varepsilon$ model by modifying the dissipation rate ε equation in order to include the effects of the different scales of motion changes into turbulent diffusion. **Initial inlet velocity fluctuating is supposed to be 5% of the mean inlet velocity V_{in}** and the turbulent kinetic energy k at the inlet is calculated as follows:

$$k = \frac{3}{2}(0.05V_{in})^2. \quad (20)$$

The turbulent dissipation rate ε is figured up by:

$$\varepsilon = \frac{C_\mu^{0.75} \times k^{3/2}}{l}, \quad (21)$$

where C_μ the is the constant and taken 0.09. l shows the characteristic length and it is set as 20% of the nozzle width W_n . Finally, turbulent viscosity μ_t is calculated as follows:

$$\mu_t = \rho_m C_\mu \frac{k^2}{\varepsilon}. \quad (22)$$

3.5. Mesh description and calculation conditions

Turbulent flow calculations are strongly affected by computational mesh, especially in the zones of the high gradients in velocity. Therefore, a mesh independency test is carried out to verify the proper mesh using three different meshes whose properties are shown in **Table 1**. We create uniform hexahedral structured grids whose smallest meshes are located in the recirculation zone using blockMesh and refineMesh utilities of OpenFOAM. **Fig. 5** shows the structured middle mesh with 73,100 hexahedral cells whose minimum cell size is 50 μm .

Fig. 6 shows the measured and calculated mean velocities at $y = -1.5, -3.0, -6.0$ mm with the combination of VOF/MR/RNG $k-\varepsilon$ when $P_{in} = 0.22$ MPa. The coarse mesh illustrated by black lines overestimates the mean stream velocity in the recirculation zone especially $x = 0-0.6$ mm, while middle mesh shown by blue and the fine mesh shown by green lines give almost identical

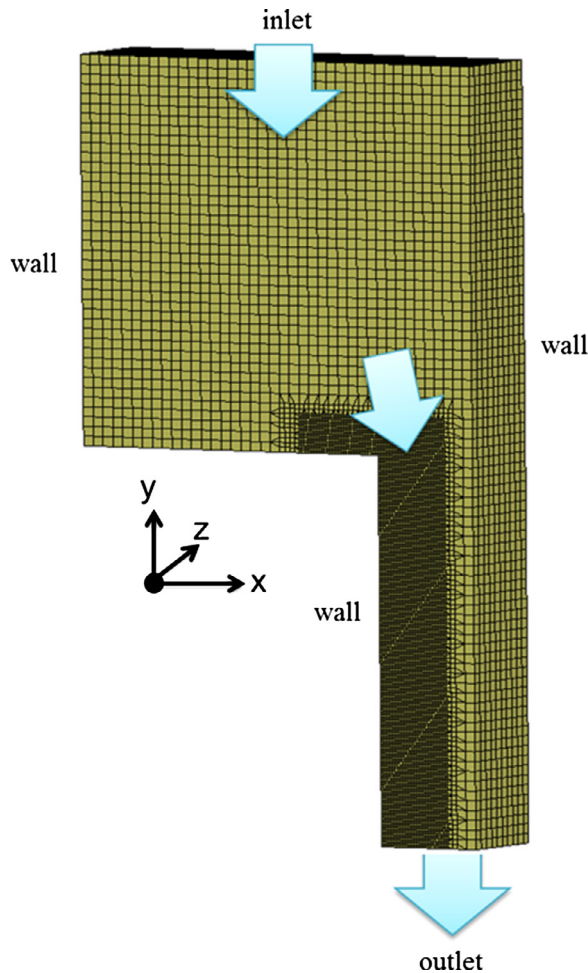


Fig. 5. 3-D computational grid (middle mesh).

Table 2
Fluid properties.

	Density, ρ (kg/m ³)	Viscosity, μ (Pa s)
Liquid (water)	998.2	1.00×10^{-3}
Vapor	1.73×10^{-2}	1.00×10^{-6}

results with the LDV measurement. Fig. 7 displays the comparison of the calculated liquid volume fraction α_L with three meshes at $P_{in} = 0.22$ MPa. Since the cavitation region changes with the time, all the simulated results are taken from same time step. As seen in the results, coarse mesh underestimates the cavitation length and thickness, and also recirculation zone, while the middle and fine meshes give almost good predictions compared to the experiment. In the view of these results and CPU time, middle mesh is chosen for the following numerical calculations.

For the calculations, an Intel Core i7 CPU X 980 @ 3.33 GHz X 6 core (each core has 2 threads), 12GB RAM PC is employed. Inlet pressure P_{in} was set to 0.22 and 0.25 MPa, while outlet pressure P_{out} was fixed to the environment pressure at 0.1 MPa. At the nozzle walls, a no-slip condition is applied. The default wall functions provided by OpenFOAM are employed for the turbulent quantities k , ϵ and ν_t . The iterative PIMPLE algorithm is used to solve pressure P and correct the mixture velocity \mathbf{U} in the solver. The second order linerUpwind scheme is chosen for the discretization of advection terms in the momentum Eq. (10), while an implicit first order Euler scheme is used for the time integration. The advection term in the transport Eq. (3) is discretized using van Leer scheme [39] without any artificial interface compression. The first order upwind scheme is used for the discretization of the convection terms of the turbulence parameters due to stability reasons. Time step Δt and the maximum Courant number are set to 10^{-8} s and 0.1, respectively. Each calculations takes approximately 2.5 days.

As a liquid, water was used in the experiment, and physical properties used in the simulations are given in Table 2. The saturation pressure P_v (= 2.3 kPa) is taken as the threshold of the cavitation for R model, while P_c is taken -31.8 and -33.2 kPa

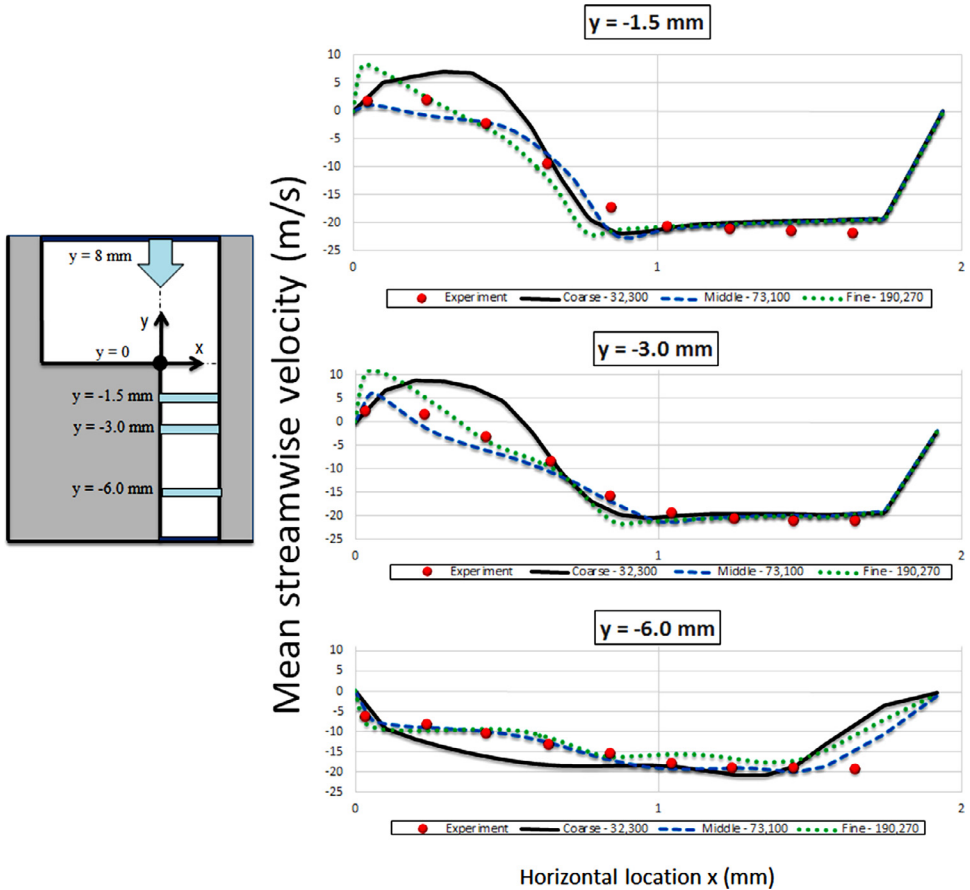


Fig. 6. Measured and calculated mean velocities at $P_{in} = 0.22 \text{ MPa}$. (For interpretation of the references to color in this figure, the reader is referred to the web version of this article).

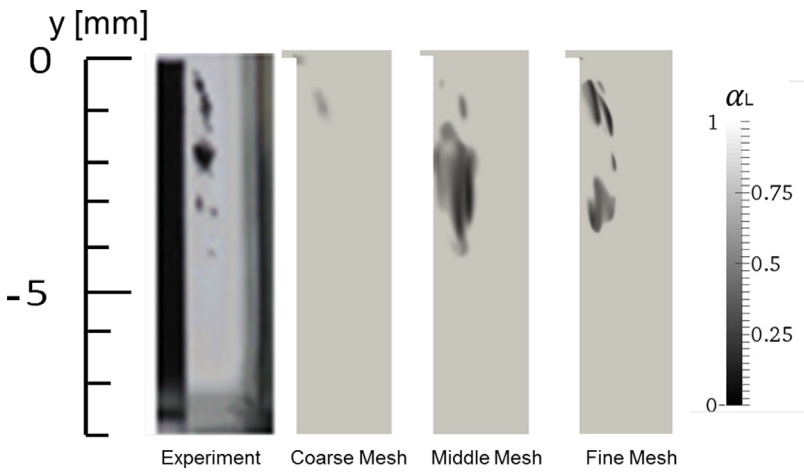


Fig. 7. Calculated liquid volume fraction with different mesh sizes ($P_{in} = 0.22 \text{ MPa}$).

(calculated according to Eq. (17)) for the MR model at P_{in} 0.25 and 0.22 MPa, respectively. Since the simulations are isothermal, these properties are constant throughout the calculations. Simulations are run in the non-cavitating condition for about 15 ms until the initial flow fields of fully developed turbulent flows are obtained. After that, the cavitation model is activated to simulate cavitation until 18 ms.

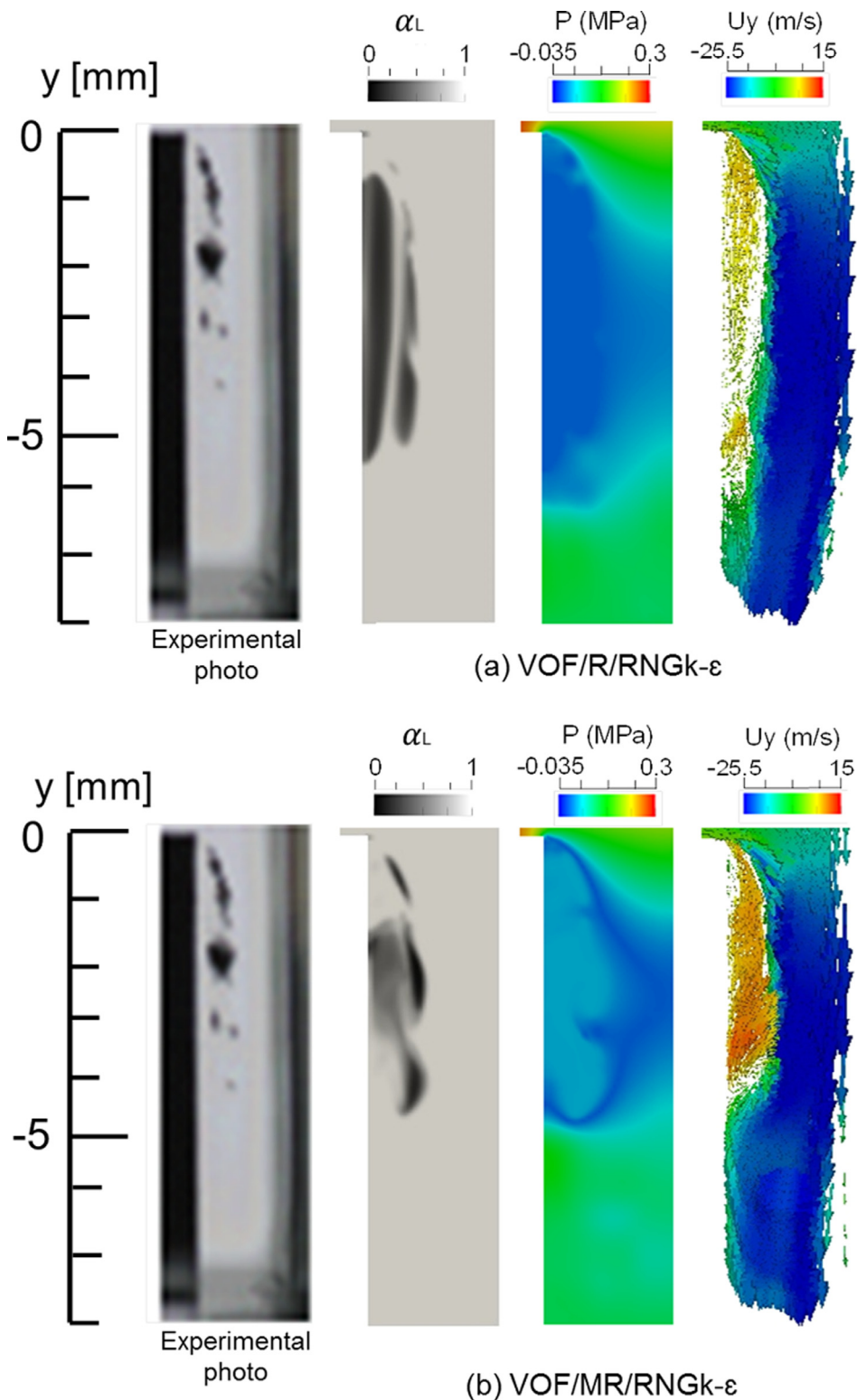


Fig. 8. Calculated cavitating flows with (a) R equation and (b) MR equation ($P_{in} = 0.22$ MPa).

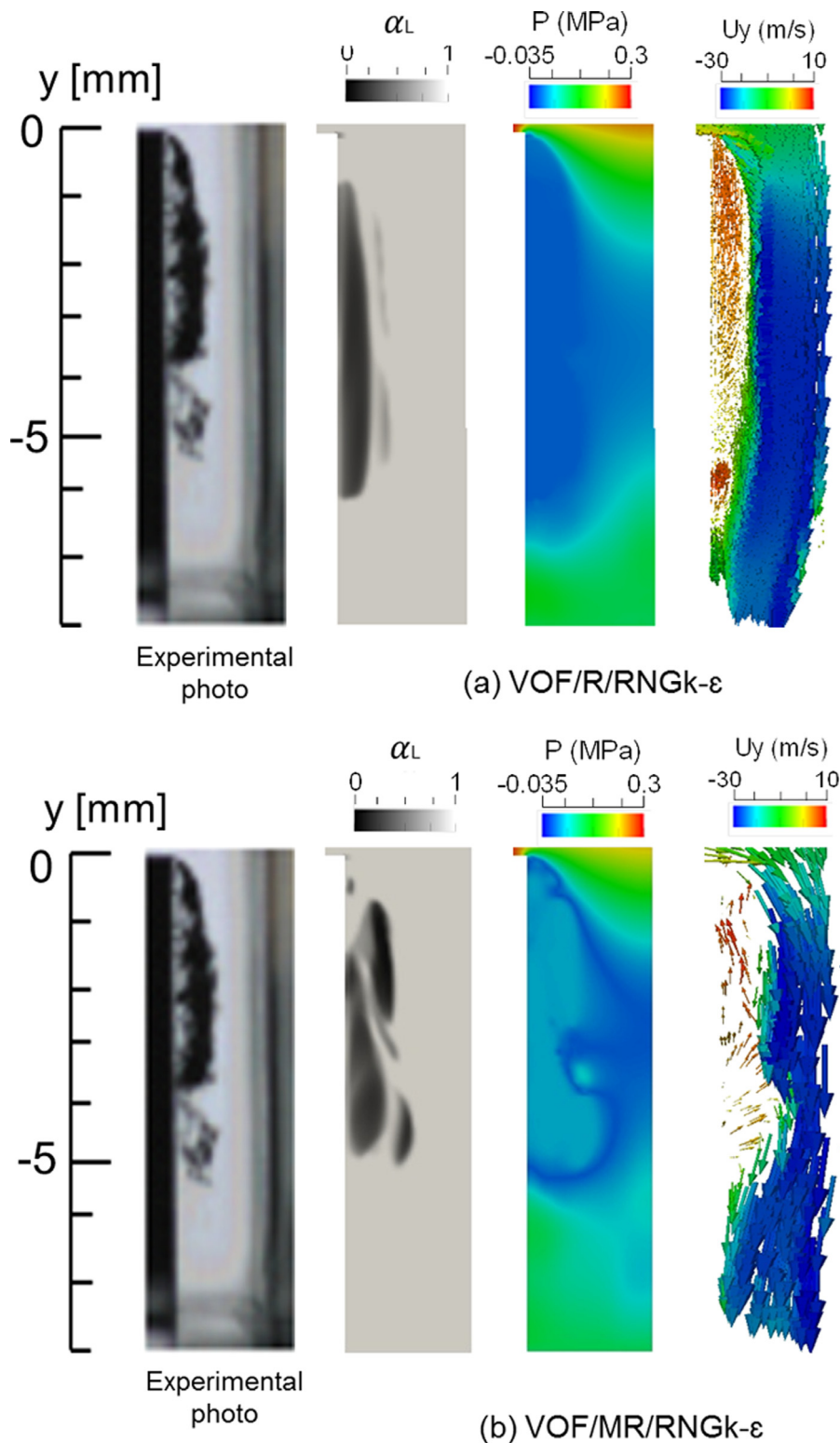


Fig. 9. Calculated cavitating flows with (a) R equation and (b) MR equation ($P_{in} = 0.25$ MPa).

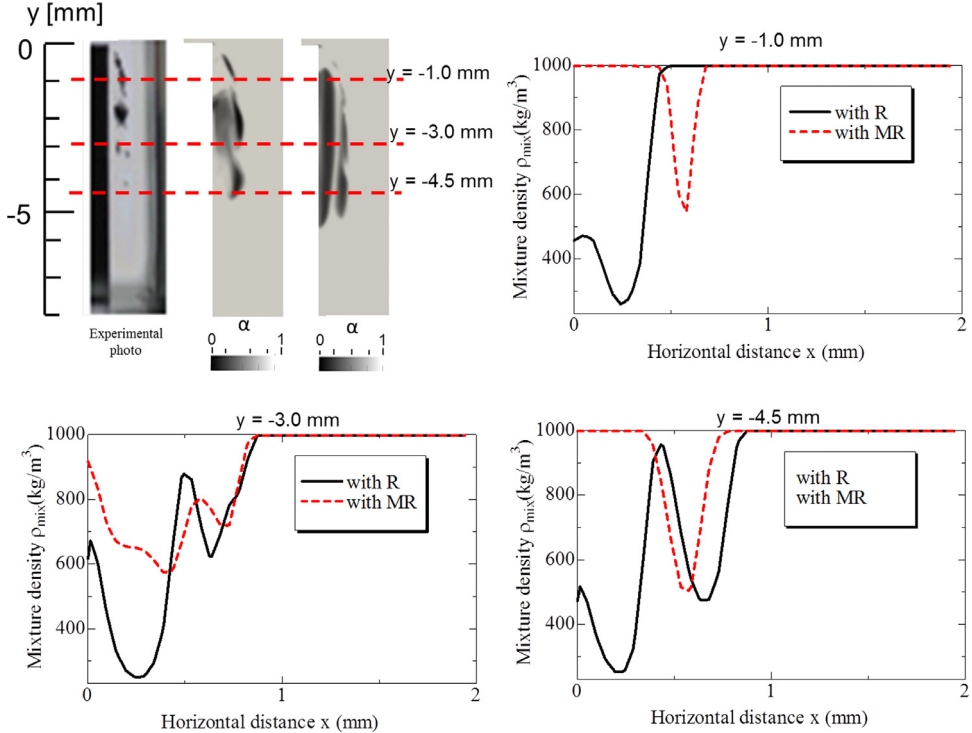


Fig. 10. Time-average density distribution over different sections of the nozzle obtained with R equation and MR equation ($P_{in} = 0.22 \text{ MPa}$).

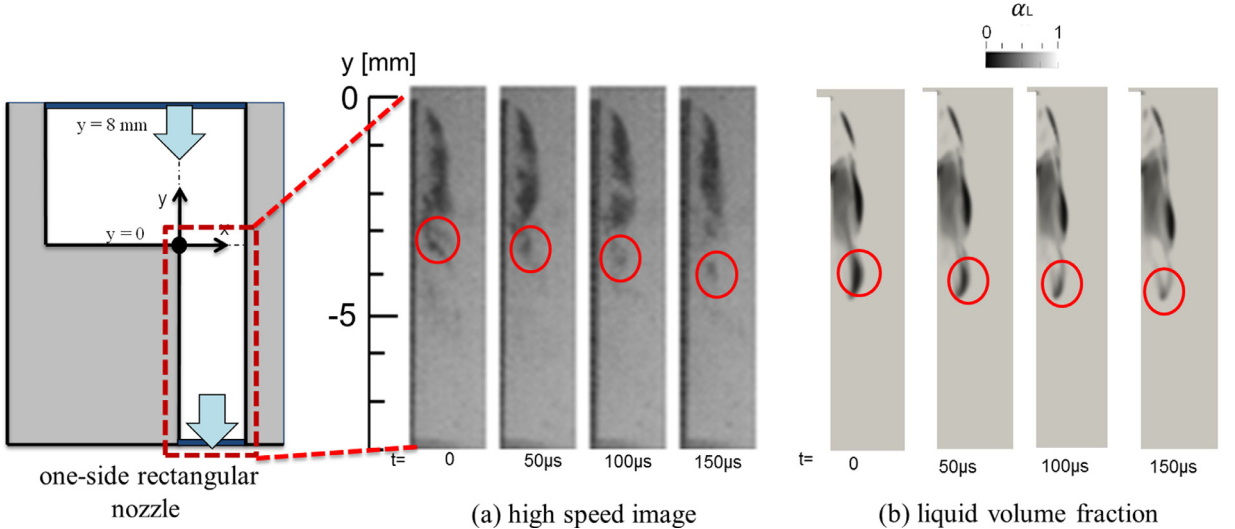


Fig. 11. Transient cavitation motion with (a) high speed image and (b) MR equation ($P_{in} = 0.22 \text{ MPa}$).

4. Results and discussion

Figs. 8 and 9 show the instantaneous results of VOF/R/RNG k- ε and VOF/MR/RNG k- ε models at $P_{in} = 0.22 \text{ MPa}$ ($K = 1.19$) and $P_{in} = 0.25 \text{ MPa}$ ($K = 0.94$), respectively. Results are illustrated in terms of liquid volume fraction α_L , pressure contours P and velocity vectors. As seen in Figs. 8(a) and 9(a), R equation over-estimates the cavitation region from the points of cavity length and thickness since cavitation takes place when the local pressure is less than the vapor saturation pressure P_v instead of critical pressure P_c . Additionally, an attached cavity without recirculation is obtained by R equation, which can be referred to the over-prediction of the turbulent viscosity, which creates high stress inside recirculation zone and damps the re-entrant jet. On the other hand, collapse of the bubble can be other reason which influences the attach cavity via turbulent spot [40]. Since both growth and collapse in R equation are treated with the same coefficient (2/3), which let the bubble collapse occur more slowly

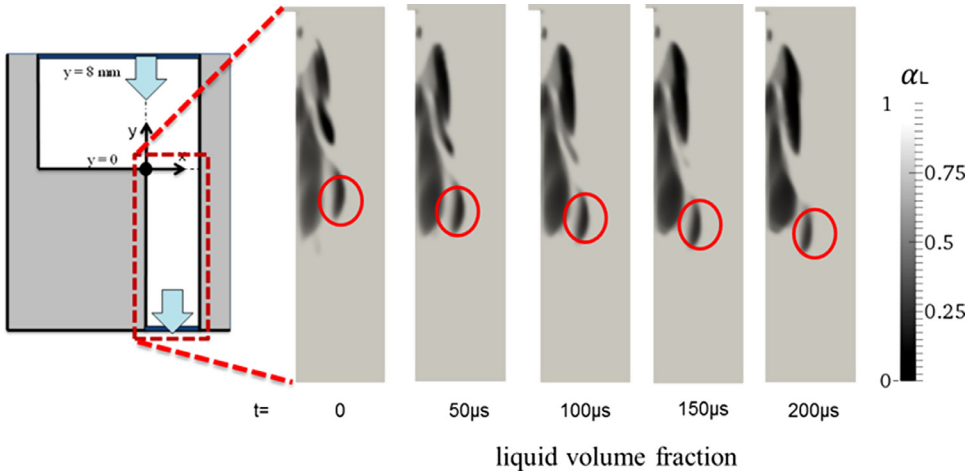


Fig. 12. Transient cavitation motion obtained with MR equation ($P_{in} = 0.25$ MPa).

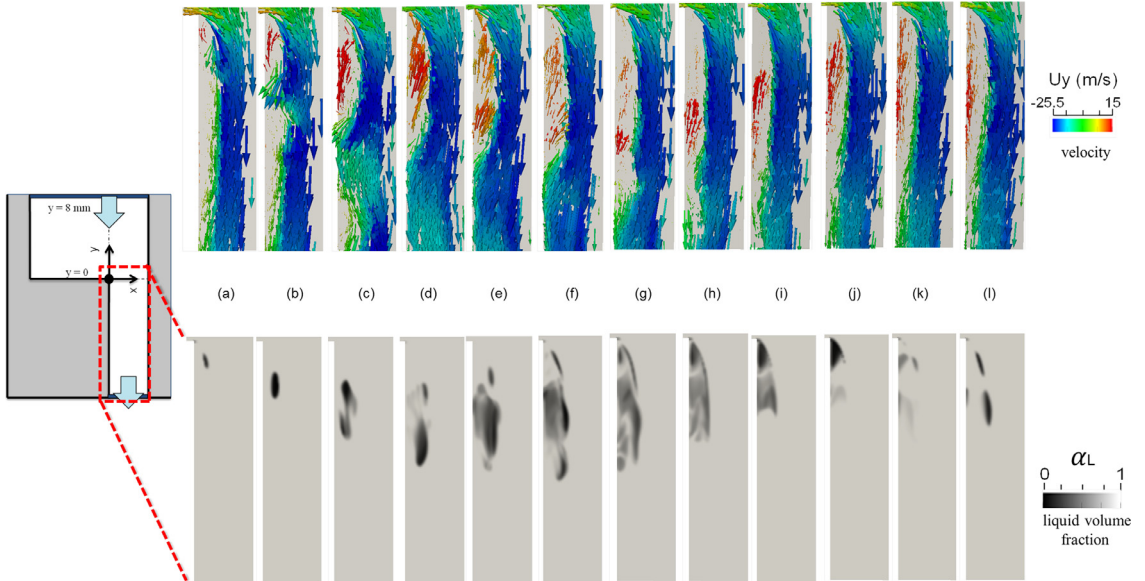


Fig. 13. Sequence of cavity cycle ($P_{in} = 0.22$ MPa, results are shown every 0.5 ms).

and cannot decrease the influence of the over-predicted turbulent viscosity in the close region of re-entrant jet. On the other hand, results obtained with MR equation based on the critical pressure P_c give better estimation with the re-entrant jet in the sense of cavity length and thickness when compared to experimental data, as shown in Figs. 8(b) and 9(b). The observation of the re-entrant jet in the results of MR equation can be attributed to modification of the collapse coefficient based on our previous work [29] from 2/3 to 1.27. Therefore, the bubble collapse can take place much faster than bubble growth, which can affect the turbulent viscosity fluctuation near the re-entrant.

This over-prediction is also seen in Fig. 10, which illustrates the time-averaged mixture density distributions in same time period calculated by R and MR equations when P_{in} is 0.22 MPa. These distributions are taken at vertical distance $y = -1.0, 3.0$ and -4.5 mm from the entrance of the nozzle, respectively. The time-averaged mixture density is calculated according to Eq. (4). As observed, model with R equation predicts that cavitation starts much earlier in comparison with MR equation due to threshold P_v . To be more accurate at $y = -1.0$ mm and -4.5 mm, model based on R equation observed that cavitation start $x = 0.0$ mm for both distance, while MR equation predicts a value of 0.42 and 0.45 mm, respectively. Experimental data gives a value of 0.40 mm and 0.42 mm. Therefore, we conclude that MR model gives better prediction for cavitation.

4.1. Transient cavitation in nozzle

Fig. 11 shows experimental high-speed images of transient cavitation and calculated cavitating flows with VOF, MR equation and RNG k- ε for $P_{in} = 0.22$ MPa. **Fig. 11(a)** is taken using the high speed camera whose time interval is 50 μ s. In the low pressure zones within the recirculation region, a huge number of nuclei grow and vortices are shed from the reattachment point. The vortex accompanied by clouds of bubbles is shed and the bubbles collapse during the shedding. The phenomena are well simulated with MR model and agreed quite satisfactorily with the high speed image. **Fig. 12** displays a good agreement in the prediction of cavitation cloud shedding with the combination of VOF/MR/ RNG k- ε when P_{in} is 0.25 MPa.

Fig. 13 illustrates a sequence of cavitation cycle with velocity vectors. These results are obtained with the combination of VOF/MR/RNG k- ε for P_{in} 0.22 MPa. The cycle begins with the small development of cavitation near the entrance of the nozzle due to sharp edge frame (a), which is called incipient cavitation. Then, cavity moves downstream and develops through the middle of the nozzle between the frames (b) and (f). The re-entrant jet induces vortex shedding (f) and shortens the cavity among the frames (g)–(j). Finally, a new cycle starts with the development of small cavity at the entrance of the nozzle, frames (k) and (l). It should be noted that the prediction of reverse flow structures and observation of the cloud shedding moving until the exit of the nozzle are limited compared to Large Eddy Simulations (LES) due to using of RANS model.

5. Conclusions

In this study, the feasibility and applicability of the Modified Rayleigh (MR) equation based on critical pressure P_c is investigated in CFD to precisely predict the cavitation region and its cloud shedding inside a nozzle. To verify the validity of the proposed model, results are compared with the conventional cavitation model based on R equation, which uses P_v as a threshold of cavitation, and experimental data. It is found out that R equation over-estimates cavitation region from the points of cavity length and thickness, while MR equation based on the critical pressure P_c gives better estimation in the sense of cavity length and thickness.

The transient motion of cavitation in the recirculation zone, such as cloud shedding, the development of the re-entrant jet and the cavity break-off is well predicted with the combination of VOF, MR and RNG k- ε . This approach is easy to be employed and applied for cavitation simulation inside nozzle since it does not need very fine grid, and therefore it has a short CPU time.

Finally, it can be stated that the combination of VOF, MR and RNG k- ε model with a proper mesh gives a fairly good prediction and can be used to obtain an insight into cavitation phenomena within a fuel injector.

References

- [1] W. Bergwerk, Flow pattern in diesel nozzle spray holes, *Proc. Inst. Mech. Eng.* 173 (1959) 655–660.
- [2] W. Nurick, Orifice cavitation and its effect on spray mixing, *ASME Trans. J. Fluids Eng.* 98 (1976) 681–687.
- [3] H. Hiroyasu, Break-up length of a liquid jet and internal flow in a nozzle, ICLASS-91, 1991 275–282.
- [4] C. Soteriou, R.J. Andrews, Direct Injection Diesel Sprays and the Effect of Cavitation and Hydraulic Flip on Atomization, SAE paper 950080, 1995.
- [5] A. Sou, S. Hosokawa, A. Tomiyama, Effects of cavitation in a nozzle on liquid jet atomization, *Int. J. Heat Mass Transf.* 50 (2007) 3575–3582.
- [6] L. He, F. Ruiz, Effect of cavitation on flow and turbulence in plain orifices for high-speed atomization, *At. Sprays* 5 (1995) 569–584.
- [7] M.E. Henry, S.H. Collicott, Visualization of internal flow in a cavitating slot orifice, *At. Sprays* 10 (2000) 545–563.
- [8] M. Daikoku, H. Furudate, H. Noda, T. Inamura, Effect of cavitation in the two-dimensional nozzle on liquid breakup process, in: Proceedings of 9th ICLASS, 2003, p. 1207.
- [9] A. Sou, B. Biçer, A. Tomiyama, Numerical simulation of incipient cavitation flow in a nozzle of fuel injector, *Comput Fluids* 103 (2014) 42–48.
- [10] D.P. Schmidt, C. Rutland, M. Corradini, P. Roosen, O. Genge, Cavitation in two-dimensional asymmetric nozzles, SAE paper, 1999 0518.
- [11] W.S. Yuan, H. Günter, Cavitation in injector nozzle - Effect of injection pressure, in: Proceedings of Fourth International Symposium on Cavitation, Pasadena, CA, June 20–23, 2001.
- [12] G. Schnerr, J. Sauer, Physical and numerical modeling of unsteady cavitation dynamics, in: Proceedings of Fourth International Conference on Multiphase Flow, New Orleans, USA, 2001.
- [13] A.K. Singhal, M.M. Athavale, H. Li, Y. Jiang, Mathematical basis and validation of the full cavitation model, *Trans.-Am. Soc. Mech. Eng. J. Fluids Eng.* 124 (2002) 617–624.
- [14] R.F. Kunz, D.A. Boger, D.R. Stinebring, T.S. Chyczewski, J.W. Lindau, H.J. Gibeling, S. Venkateswaran, T.R. Govindan, A preconditioned Navier–Stokes method for two-phase flows with application to cavitation prediction, *Comput. Fluids* 29 (2000) 849–875.
- [15] P.J. Zwart, A.G. Gerber, T. Belamri, A two-phase flow model for predicting cavitation dynamics, in: Proceedings of Fifth International Conference on Multiphase Flow, Yokohama, Japan, 2004.
- [16] A. Alajbegovic, D. Greif, B. Basara, U. Iben, Cavitation calculation with the two-fluid model, in: Proceedings of 3rd European-Japanese Two-phase Flow Group Meeting, 21–27 September, 2003.
- [17] E. Giannadakis, M. Gavaises, C. Arcoumanis, Modelling of cavitation in diesel injector nozzles, *J. Fluid Mech.* 616 (2008) 153–193.
- [18] C.L. Merkle, J. Feng, P.E. Beulow, Computational modeling of the dynamics of sheet cavitation, in: Proceedings of 3rd International Symposium on Cavitation, 2, Grenoble, France, 1998, pp. 47–54.
- [19] N. Dumont, O. Simonin, C. Habchi, Numerical simulation of cavitating flows in diesel injectors by a homogeneous equilibrium modeling approach, in: Proceeding of CAV2001: sessionB6. 005, 2001.
- [20] B. Charriere, J. Decaix, E. Goncalves, A comparative study of cavitation models in a Venturi flow, *Eur.J. Mech.–B/Fluids* 49 (2015) 287–297.
- [21] E. Goncalves, R.F. Patella, Numerical simulation of cavitating flows with homogeneous models, *Comput. Fluids* 38 (2009) 1682–1696.
- [22] F. Salvador, J.-V. Romero, M.-D. Roselló, J. Martínez-López, Validation of a code for modeling cavitation phenomena in Diesel injector nozzles, *Math. Comput. Model.* 52 (2010) 1123–1132.
- [23] V. Srinivasan, A. Salazar, K. Saito, Computational prediction of the flow inside cavitating injectors by supplementing a homogeneous equilibrium model (HEM) with a pressure correction equation, in: Proceedings of the International Conference on Liquid Atomization and Spray Systems (ICLASS 2006), Kyoto, Japan, 2006.
- [24] B. Biçer, A. Tanaka, T. Fukuda, A. Sou, Numerical Simulation of Cavitation Phenomena in Diesel Injector Nozzles, in: Proceedings of the 16th Annual Conference of Institute for Liquid Atomization and Spray Systems, ILASS-ASIA, Nagasaki-JAPAN, 2013, pp. 58–65.
- [25] Y. Delannoy, J. Kueny, Two phase flow approach in unsteady cavitation modelling, *Proc. Cavitation Multiph. Flow Forum* 98 (1990) 153–158.
- [26] F.P. Kärholm, H. Weller, N. Nordin, Modelling Injector Flow Including Cavitation Effects for Diesel Applications, ASME, 2007.
- [27] C.W. Hirt, B.D. Nichols, Volume of fluid (VOF) method for the dynamics of free boundaries, *J. Comput. Phys.* 39 (1981) 201–225.

- [28] L. Rayleigh VIII, On the pressure developed in a liquid during the collapse of a spherical cavity, *Lond. Edinb. Dublin Philos. Mag. J. Sci.* 34 (1917) 94–98.
- [29] B. Bicer, A. Sou, Bubble dynamics model for predicting the growth and collapse of the cavitation bubbles in diesel injector, *At. Sprays* 24 (2014) 915–935.
- [30] C. Deimel, M. Günther, R. Skoda, Application of a pressure based CFD code with mass transfer model based on the Rayleigh equation for the numerical simulation of the cavitating flow around a hydrofoil with circular leading edge, *EPJ Web Conf. EDP Sci.* 67 (2014) 02018.
- [31] A. Gosset, M. Lema, F.L. Peña, Periodic phenomena on a partially cavitating hydrofoil, in: Proceedings of the Eighth International Symposium of Cavitation, 2012, pp. 685–690.
- [32] M. Morgut, E. Nobile, I. Biluš, Comparison of mass transfer models for the numerical prediction of sheet cavitation around a hydrofoil, *Int. J. Multiph. Flow* 37 (2011) 620–626.
- [33] S.E. Kim, A numerical study of unsteady cavitation on a hydrofoil, in: Proceedings of the 7th International Symposium on Cavitation, Ann Arbor, MI, USA, 2009 Paper No. 56.
- [34] E. Roohi, A.P. Zahiri, M. Passandideh-Fard, Numerical simulation of cavitation around a two-dimensional hydrofoil using VOF method and LES turbulence model, *Appl. Math. Model.* 37 (2013) 6469–6488.
- [35] Z. Shang, D.R. Emerson, X. Gu, Numerical investigations of cavitation around a high speed submarine using OpenFOAM with LES, *Int. J. Comput. Methods* (2012) 9.
- [36] Y.L. Young, B.R. Savander, Numerical analysis of large-scale surface-piercing propellers, *Ocean Eng.* 38 (2011) 1368–1381.
- [37] J.P. Franc, Physics and Control of Cavitation, DTIC Document, 2006.
- [38] V. Yakhot, S. Orszag, S. Thangam, T. Gatski, C. Speziale, Development of turbulence models for shear flows by a double expansion technique, *Phys. Fluids A: Fluid Dyn.* (1989–1993) 4 (1992) 1510–1520.
- [39] B. Van Leer, Towards the ultimate conservative difference scheme. IV. A new approach to numerical convection, *J. Comput. Phys.* 23 (1977) 276–299.
- [40] M.L. Briancon, J.P. Franc, J.M. Michel, Transient bubbles interacting with an attached cavity and the boundary layer, *J. Fluid Mech.* 218 (1990) 355–376.